ACTA UNIVERSITARIA
Multidisciplinary Scientific Journal

| VOLUMEN 29 | 2019 |
ISSN online 2007-9621
http://doi.org/10.15174/au.2019.2351

Microstructure and mechanical properties of AISI 439 ferritic stainless steel welds without filler metal

Microestructura y propiedades mecánicas de soldaduras de acero inoxidable ferrítico 439 sin metal de aporte

Juan Manuel Salgado Lopez[1]*, Marc Preud´homme[1], Francisco López Monroy[1], José Luis Ojeda Elizarráraz[1], Arturo Toscano Giles[2].

[1] Laboratorio de metalografía y análisis de falla, Tecnología de materiales, Centro de Ingeniería y Desarrollo Industrial. Querétaro, México. Av. playa pie de la cuesta No.702, Querétaro, México. C.P. 76125. *Correo electrónico: msalgado@cidesi.edu.mx

[2] Instituto Tecnológico de Querétaro. Posgrado e investigación, México.

*Autor de correspondencia

Abstract

In literature, it has been reported that a current intensity lower than 120 A leads to a microstructure without grain growth in the heat affected zone (HAZ) of ferritic stainless steel welds. Nevertheless, in technical literature there is little information about the reduction in mechanical properties of ferritic stainless steel welds without filler metal due to grain growth in the HAZ. In this work, thin plates of ferritic stainless 439 steel were welded using pulse current gas tungsten arc welding (P-GTAW) without filler metal. The microstructures in the HAZ were analyzed and the mechanical properties on the welded joint were found by tensile test. This was carried out by cutting samples for the tensile test from the weldments and then tested in a universal testing machine. The fracture surface were observed using scanning electron microscope.

Keywords: Properties; microstructure; grain growth; ferritic stainless steel; welding.

Resumen

En la literatura sobre soldadura de acero inoxidable ferrítico ha sido reportado que una intensidad de corriente de soldadura menor a 120 A da lugar a una microestructura sin crecimiento de grano en la zona afectada térmicamente (ZAT). No obstante, en la literatura técnica existe muy poca información acerca de la reducción en las propiedades mecánicas de las uniones soldadas de acero AISI 439, usando el proceso de soldadura de arco con electrodo de tungsteno con corriente pulsada sin metal de aporte (P-GTAW, por sus siglas en inglés). En este trabajo, las microestructuras en la ZAT fueron analizadas y las propiedades mecánicas determinadas por ensayo mecánico a la tensión. Esto fue hecho en muestras cortadas para ensayo de las uniones soldadas y ensayadas en una máquina de ensayos universal. Las superficies de fractura fueron observadas utilizando microscopia electrónica de barrido.

Palabras clave: Propiedades; microestructura; crecimiento de grano; acero inoxidable ferrítico; soldadura.

Recibido: 3 de agosto de 2018 Aceptado: 13 de noviembre de 2019 Publicado: 11 de diciembre de 2019

Como citar: Salgado-Lopez, J. M., Preud´homme, M., López-Monroy, F., Ojeda-Elizarráraz, J. L., & Toscano-Giles, A. (2019). Microstructure and mechanical properties of AISI 439 ferritic stainless steel welds without filler metal. *Acta Universitaria 29*, e2351. doi. http://doi.org/10.15174.au.2019.2351

BY-NC-ND

Introduction

Ferritic stainless steel (FSS) is important in modern industry because of its low cost, relatively good mechanical properties, good stress corrosion cracking resistance, etc. However, its weldability is still an issue (Khattak *et al*., 2017). After an exhaustive search in the technical literature, little information about welding of FSS was found. This is especially true in the case of welding FSS without filler metal and its final mechanical properties. Therefore, this work was carried out in order to provide information about the mechanical properties of AISI 439 AISI welds without filler metal using gas tungsten arc welding (GTAW) (Amuda, Akinlabi & Mridha, 2017; Amuda & Mridha, 2010; Khattak *et al*., 2017). This process was chosen because it is applied to weld ferritic stainless steel plates without filler metal.

In literature it has been reported that one of the main problems that occur with FSS welding is grain coarsening in the HAZ (Amuda & Mridha, 2010; Khattak *et al*., 2017). For instance, GTAW welding is applied to AISI 439 in the manufacturing of exhaust systems in the automotive industry. The process induces heat to the material, which causes grain growth in the HAZ of the FSS. This phenomenon is called grain coarsening. When the grain size of the HAZ is higher than the average grain size of the base material, the mechanical properties are lower in this area than in the rest of the component. This reduction in mechanical properties is a problem in FSS because they are not homogeneous through the whole material, and it induces failure in the HAZ.

In 2017, Amuda, Akinlabi & Mridha reported that low heat inputs with welding intensities and titanium or niobium in the base metal lead to microstructures without grain growth in AISI 430 stainless steel. They have related microstructures in the HAZ with different welding parameters (Amuda *et al*., 2017; Amuda & Mridha, 2010).

Azevedo *et al.* carried out a microstructural characterization of the HAZ of AISI 439 welded with different heat input using gas metal arc welding (GMAW). They found grain growth and precipitates in the HAZ (Silva, Lima, & Campos, 2007).

Zaman, Khattak & Tamin (2018). published a work about the microstructure and mechanical properties of AISI 430 welded using GTAW. They found a change in microstructure of the weld deposit in comparison with the fine equiaxial grains of the base metal (Zaman *et al*., 2018).

Mohandas, Reddy & Naveed (1999) researched the microstructure and mechanical properties in weldments of AISI 430 with different shielding gases (Mohandas *et al*., 1999). In the same way, Lakshminarayanan & Balasubramanian (2012) published their work about welding of AISI 409 stainless steel. In this work they welded AISI 409 using laser beam welding. They concluded that, despite of the low grain growth, the tensile properties were higher than the base materials. In a previous work by the same authors they researched AISI 409 stainless steel welded without filler metal using different autogenous arc welding processes and concluded that, in comparison with other processes, plasma arc welding generates the best mechanical properties due to the lower heat input (Lakshminarayanan, Shanmugam & Balasubramanian, 2009). But their results are not comparable to AISI 439 stainless steels because of the difference in carbon content. It must be kept in mind that this research was carried out in ferritic stainless steel containing much more carbon than AISI 439; therefore, the results of the mechanical properties are different and their conclusion was that GTAW is the best welding process for ferritic 409 stainless steel, but the HAZ showed grain growth, regardless the welding process (Lakshminarayanan & Balasubramanian, 2012; Lakshminarayanan, *et al*., 2009).

Ramkumar *et al.* (2015) carried a comparative study of tensile properties and microstructure in AISI 430 welded with and without flux. They found high mechanical properties welding using Fe_2O_3 as flux and evidence of martensite in HAZ microstructures. However, their research focused on welding with filler metal (Ramkumar *et al*., 2015).

In 2015, Zhang *et al.* reported the microstructure evolution in T4003 FSS, which is a stainless steel with a 12% of chromium and titanium as a stabilizing element. They concluded that the hardness profile and microstructures distribution

indicated that HAZ can be divided into three distinct metallurgical transformation zones and they found an inconspicuous grain coarsening in the HAZ1 of T4003 steel (Zhang *et al*., 2015).

Villafuerte, Kerr & David (1995) did a research on the effect of the chemical composition to get equiaxial grains in FSS weld metal. They concluded that minor elements such as Ti or Al reduce the grain size and play a role for the generation of columnar grains in the weld metal. However, the authors focused their research on the weld metal, and they did not give information about the HAZ (Villafuerte *et al*., 1995).

Amuda & Mridha (2009) found that low heat inputs with welding intensities lower than 120 A lead to good microstructures in the HAZ of AISI 430; they related microstructures in the HAZ with different welding parameters. Besides, they concluded that average heat inputs produced the better microstructures in HAZ, and they generated the better mechanical properties of the welds. However, they did not carry out any mechanical testing (Amuda & Mridha, 2009).

Anttila & Porter (2014) reported the microstructures and properties after welding in many ferritic stainless steels, which were welded using metal active gas welding with filler metal. In the case of AISI 409, they reported a hardness decay in the HAZ respecting the base material or the weld metal. In fact, they found that using filler metals with titanium in the welding process gives place to a final microstructure in the weld metal consisted of fine columnar grains with a hardness like the base material. However, they did not weld the FSS using GTAW without filler metal (Anttila, Karjalainen & Lantto, 2013; Anttila & Porter, 2014).

From the literature reviewed, it was clear that there is little information about AISI 439 ferritic stainless steel welding using GTAW without filler metal. So then, due to the need of information about the relation between mechanical properties and GTAW welding parameters of FSS joined without filler metal, the objective of this work is to report the mechanical properties and the microstructures of AISI 439 FSS welded without filler metal and using GTAW with different welding currents, which have been reported in literature as the best choice for this material.

Materials and methods

The welding process applied in this work was automatized pulsed current Gas Tungsten Arc Welding (P-GTAW) with high purity argon (99.999% of purity) as shielding gas. This process was chosen because it generates low heat inputs, and the theory establishes that a low heat input leads to lower grain coarsening. In figure 1 it is shown the protection chamber, which was applied during the welding of the AISI 439 in this work. The welding parameters are shown in table 1. In the technical literature similar values to the ones chosen here have been reported as the ones that generate the best microstructures (Amuda & Mridha 2010; Silva *et al*., 2007; Zaman *et al*., 2018). Therefore, such values were applied in this work.

ISSN online 2007-9621

Figure 1. Protection chamber used during welding the FSS of this research.
Source: Author's own elaboration.

Table 1. Welding parameters for P-GTAW.

Sample	Welding speed (mm/s)	Welding current (A)	Welding potential (V)	Frequency (Hz)	Heat input (J/mm)
1	2.54	55	10.8	20	210.47
2	2.54	75	10.8	20	287.01
3	2.54	85	10.8	20	289.13
4	2.54	45	10.8	20	172.20
5	2.54	60	10.8	20	229.61

Source: Author's own elaboration.

The original plate of AISI 439 FSS was cut to get samples with the following dimensions: 160 mm × 50 mm × 5.10 mm. These plates were the base materials for the weldments of this work. The typical chemical composition of this material is shown in table 2, but the chemical composition was verified by quantitative chemical analysis with an optical emission spectrometer Espectrolab LaV MB 18B, SPECTRA A220, and the elements are indicated by their names.

The plates were butt welded along the 160 mm length. In figure 2, one of the GTAW welded specimens is shown. Four samples of each welding condition were made and each specimen was visually tested. Besides, the bending test was carried out on samples taken from all welded specimen to evaluate the soundness of the welds. This test was carried out following ASTM E190-14 in order to determine the best weld conditions, which were used to cut samples for tensile test and metallography. From these results, the best samples were chosen for metallographic analysis following ASTM-E03-11. Specimens of the best weld conditions were prepared for metallographic testing. Samples were cut from the weld specimens and prepared for metallography following ASTM-E03-11. The microstructures were revealed by chemical etching, which was carried out with Vilella's etchant (American Society of Testing Materials, 2011). The observation was made with a NIKON EPIPHOT 200 optical microscope with image analyzer.

ISSN online 2007-9621

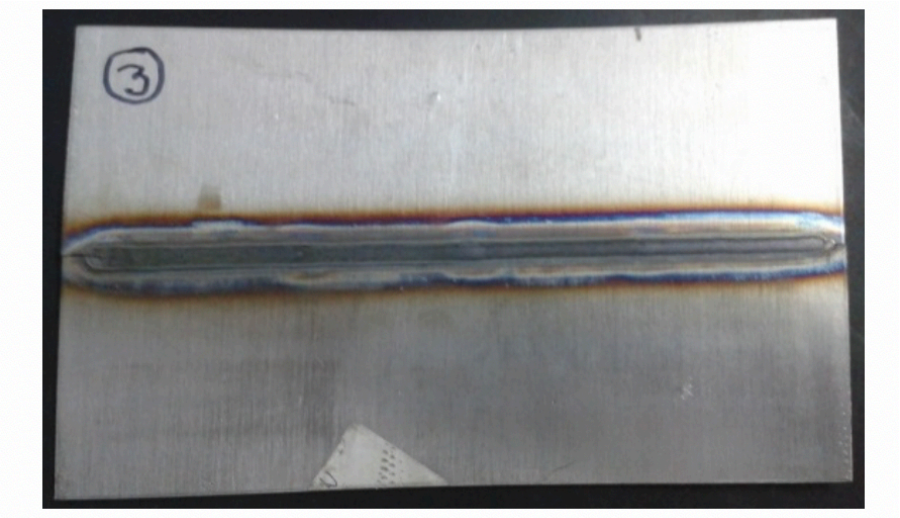

Figure 2. Welded specimen using GTAW.
Source: Author's own elaboration.

The welded specimens that withstood bending test and with the best microstructures were selected and cut to obtain tensile test specimens following ASTM-E08-16 (American Society of Testing Materials, 2016). The specimens were tested using an INSTRON universal testing machine following the same standard. It must be mentioned that the tensile axes of the samples were perpendicular to the weld of the specimen and the elongation during each tensile test was measured until 1% of unit deformation using a B class extensometer. Three samples of each welding condition were tested and the average mechanical properties are reported in table 3.

The fracture surfaces of the tensile test specimens were inspected using a Scanning Electron Microscope JEOL JSM 6610LV. This is very important because a ductile material is a requirement for welded FSS components that are deformed after welding.

Results

The results obtained in this work are shown in this section. It is worth mentioning that samples with defects, such as lack of fusion, were rejected for mechanical testing.

The chemical composition obtained by quantitative chemical analysis is shown in table 2. It indicated that the base materials matched with the nominal chemical composition of an AISI 439 ferritic stainless steel.

By visual inspection carried out on all the samples, only sample 4 had a flaw, which consisted in an incomplete penetration in the root of the weld metal, as shown in figure 3. This fact eliminates this specimen for next tests and inspections.

The evidence obtained through metallographic analysis indicated that sample 1, which was welded using automatized P-GTAW, showed low grain growth in the HAZ. However, an incomplete fusion in the weld metal was also found in it. The lack of fusion detected by visual testing is shown in figure 3. This fact was confirmed by fractography on the fracture surface of this sample. As it was performed previously, this specimen was eliminated for the next inspections.

ISSN online 2007-9621

Table 2. Results of the chemical analysis in the base material.

Element	AISI 439	Results of laboratory
Carbon	0.07% max.	0.02%
Silicon	1.0%max.	0.38%
Phosphorus	0.04% max.	0.02%
Manganese	1.0% max	0.27%
Sulfur	0.030% max.	>0.003%
Nickel	0.50% max	0.18%
Chromium	17.0% – 19.0%	17.3%
Aluminum	0.15%	0.02%
Titanium	12 x C -1.1%	0.34%
Copper	Not indicated	0.14%
Vanadium	Not indicated	0.12%

Source: Author's own elaboration.

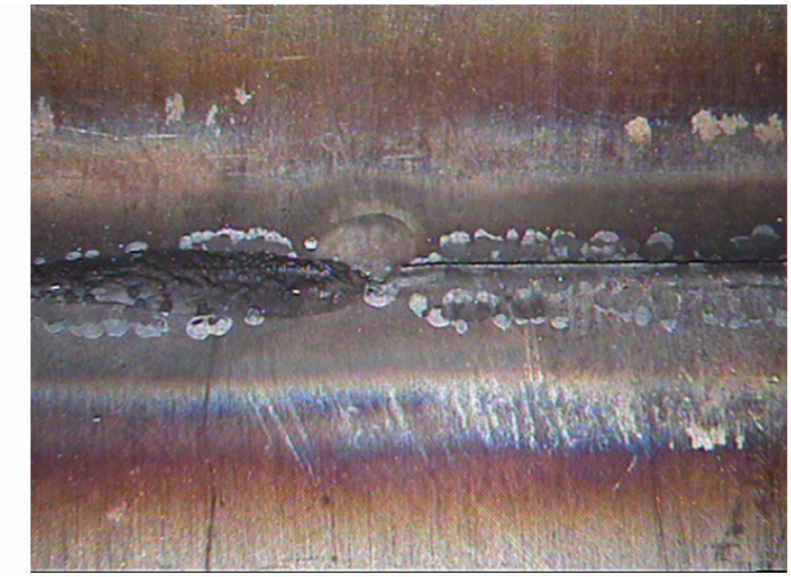

Figure 3. Visual testing on the root welding of sample 1. It can be seen a lack of fusion.
Source: Author's own elaboration.

In figure 4, it is observed the microstructure in the HAZ of sample 1 (figure 4). It is clear a lower grain coarsening compared to sample 3 (figures 5), where the grains are bigger and the lack of fusion in sample 1 is clear. Despite of the fact that all samples showed grain coarsening, the HAZ of sample 3 had the lowest grain coarsening among the samples without flaws (figure 5). In the same way, in the microstructures of samples was not observed evidence of martensite needles at the grain boundaries. Also, in figures 4 and 5 it is observed that the grain size is not homogeneous. Moreover, the grains in the HAZ are recrystallized or partially recrystallized, while in the base metal the grains are deformed. The micrographs showed a mixture of grain sizes along the HAZ of the samples, then it was not possible to define a region of the HAZ where no mix of grain sizes was found. Then, the grain sizes in the HAZ of the samples were not measured because ASTM 112-13 indicates that no attempt for measuring partially recrystallized grain size shall be carried out (American Society of Testing Materials, 2013).

ISSN online 2007-9621
Salgado-Lopez, J. M., Preud´homme, M., López-Monroy, F., Ojeda-Elizarráraz, J. L., & Toscano-Giles, A.
Microstructure and mechanical properties of AISI 439 ferritic stainless steel welds without filler metal | 1-12

Figure 4. Microstructure of sample 1 at 100X.
Source: Author's own elaboration.

Figure 5. Microstructure of sample 3 at 100X.
Source: Author's own elaboration.

The welded specimens were tensile tested and the mechanical properties determined. The results are shown in table 3. It must be pointed out that there is not a standard test for ductility. Therefore, in this work, elongation is considered as a measurement of ductility. The mechanical properties of the base material were also measured, because they were used as reference for comparison. They are denominated in table 3 as BM. This was done so, because the best mechanical properties of a weld are the most similar ones to the base material. In other words, the more similar the mechanical properties of the weld are to the mechanical properties of the base metal, the better the mechanical behavior is.

The bend test was carried out in all samples, but sample 4 was the only one that failed in this test. Figure 6 shows the specimens of sample 4 after bending test. This specimen was discarded for mechanical testing because no welded joint was obtained even after several tries. It can be seen that the fractures of the sample were located in the weld seam, and they resembled brittle fracture because no evidence of deformation was found. However, in order to confirm the fracture mode, the fracture surfaces were inspected using scanning electron microscope (SEM). These results agreed with and confirmed the metallographic analysis where lacks of fusion in some areas of the weld were found.

Table 3. Mechanical properties of the samples.

ID	Ultimate tensile strength (MPa)	Yield strength (MPa)	% Elongation (%)	UTS SD	Yield strength SD	Elongation SD
BM	474.82	322.90	33.00	1.276	1.282	0.327
1	453.58	283.73	28.93	2.335	13.45	0.170
2	374.23	300.04	25.06	25.990	2.401	0.239
3	457.71	288.99	29.98	5.17	14.81	0.266
5	446.73	298.91	28.26	8.305	5.401	0.812

Source: Author's own elaboration.

ISSN online 2007-9621

Figure 6. Bend test specimens of sample 1 after being tested.
Source: Author's own elaboration.

The fracture of the tensile specimens of samples 3, 5 and the base material showed dimples as fracture pattern. As an example, in figure 7 the fracture surface of sample 3 can be seen. It can also be seen dimples and deformation of the edges of the specimen. This pattern indicates a ductile fracture which is consistent with the results previously discussed.

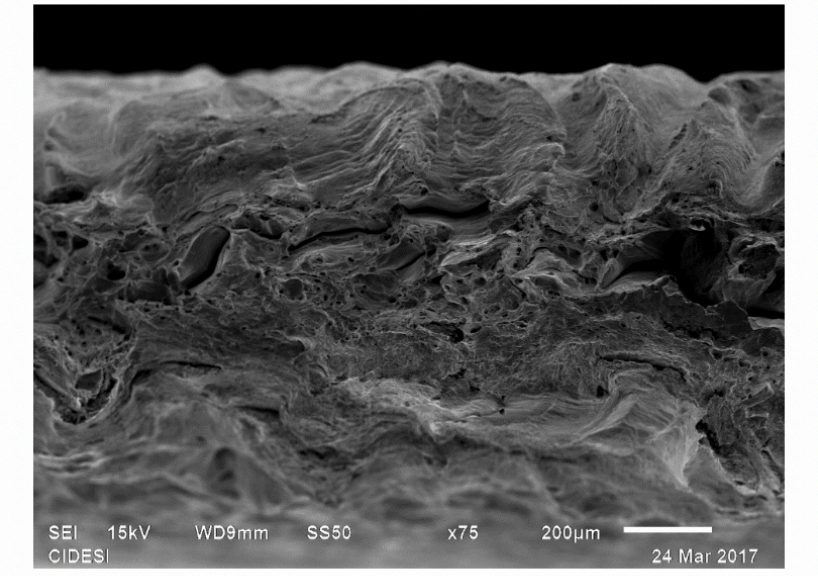

Figure 7. The image shows the fracture surface of sample 3.
Source: Author's own elaboration.

On the other hand, the pattern of the fracture surface in sample 4 consisted in cleavage, and a lack of fusion is seen on it. These facts are shown in figure 8, and they also match with the metallographic analysis and the mechanical properties. It was interesting to find cleavage on the fracture surface of this sample, because evidence was detected on the fracture surfaces of other samples. For instance, sample 1 showed cleavage on the fracture surface, which is a mix of dimples and cleavage.

ISSN online 2007-9621

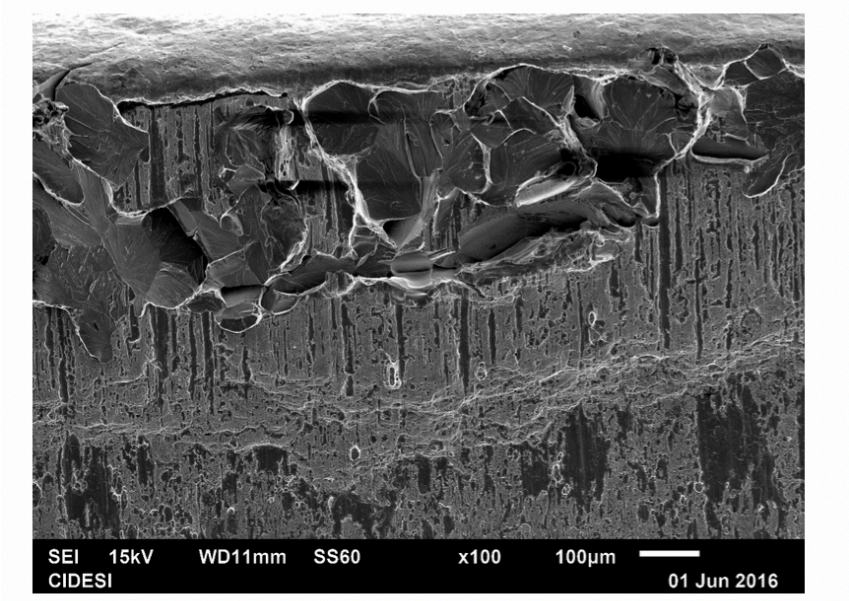

Figure 8. Fracture surface of sample 4.
Source: Author's own elaboration.

Discussion

From chemical analysis, the results showed that the chemical composition matched with the standard. It must be pointed out that the copper and vanadium content of the base material were determined and showed in table 2, because these elements have an influence in the behavior of the material during the welding process. The results indicated that the titanium content is higher than the nominal content indicated in the standard. It must be clear that this element as well as vanadium are strong carbide formers, and then it is feasible that the excess of these elements helps to avoid grain coarsening. It is also clear that the amount of phosphorus and sulfur is very low, then no harmful influence of such elements is expected after welding either (Wright, 1971). In the same way, the low carbon content induces to think that the HAZ of this steel will be free of martensite. This fact was confirmed by metallographic analysis.

Visual testing on the samples showed evidence of lack of fusion on the welding root in samples 1 and 4. But the most critical was in sample 1. In literature, it has been explained that this flaw is caused by a welder's lack of skill or low heat inputs (Sathish, Naveen, Nijanthan, Geethan & Rao, 2012). In this case, the welding process was carried out in an automatized system and, therefore, the cause of this flaw was attributed to a low heat input. This statement agrees with the fact that these samples were welded using the lowest heat input of the automatized P-GTAW process. Once again, the latter is agrees with the information reported in the literature, where it has been stated that a low heat input produces defects in welds, which are causes for rejection (Chandrakanth, Abinesh, Ashwin & Sathish, 2014; Sathish *et al.*, 2012; Teker, 2013; Wright,1971).

From the tensile test, it is shown that, as opposed to the FSS welds with filler metals reported in the literature, all samples of the present work fractured in the weld deposit. This can be explained by the fact that filler metals have alloying elements that refines the microstructures and improved the mechanical properties of the weld metals, but this is in contrast to the welds without filler metal of this work. So, from table 3 it is clear that sample 3 had the best mechanical properties. This was considered so, because those values are similar to the mechanical properties of the base metal and the elongation is the highest (29.98%). This sample was welded with a heat input of 295.28 J/mm.

In the case of elongation, again sample 3 had the highest values of elongation, and it is similar to the elongation of the base metal. In other words, these welding conditions lead to welded joints with good ductility and they might be able to be formed after welding. Sample 1 had also a high elongation but, due to its lower ultimate tensile strength, it is considered to not be the best option for deformation after welding. The fracture surface of sample 3 showed dimples, which indicated a ductile behavior of the sample during the test (figure 7). This fact matched with the result of elongation measured through tensile test and the results reported in literature.

In the same table 3, it is clearly observed that sample 1 had a brittle behavior during the test. Therefore, it has the worst properties compared the base material. In fact, the sample showed embrittlement and a lack of fusion (figure 7). This evidence was confirmed by fractographic analysis and it indicated that the welding parameters applied for sample 8 are not the best option for welding FSS AISI 439.

In this way, literature has explained that embrittlement of FSS welds, which is represented by cleavage on the fracture surface, is induced by elements such as titanium or copper in the filler metals (Khattak *et al*., 2017; Lakshminarayanan *et al*., 2009; Villafuerte *et al*.,1995). In this work, no filler metal was applied in the weld, but the percentage of titanium and copper is relatively high in the base material; then, it is feasible that the cleavage found in some samples of this work was caused by segregation of copper or titanium. These facts agree with the results reported in the literature, because low heat inputs induce defects and low grain coarsening in the HAZ (Khattak *et al*., 2017; Lakshminarayanan *et al*., 2009). In this way, it can be stated that in the case of welds without filler metal, the best heat input is the one that does the balance between the loss of mechanical properties due to grain coarsening and the need of getting welds without incomplete fusion in the weld metal, in this case, a heat input of 295.28 J/mm.

In the case of the microstructural analysis, the microstructures showed no evidence of laves phases nor martensite. However, grain growth was found in all microstructures. This has been reported in the HAZ of FSS by authors as Amuda *et al.* (2017) or Zaman *et al.* (2018) (Amuda & Mridha, 2010, Silva, *et al*., 2007; Teker, 2013; Wright,1971; Zaman *et al*., 2018), but one has to bear in mind that they work with different steels and using filler metals. Nevertheless, similar microstructures have been also reported by Amuda & Mridha (2009) for similar heat inputs. However, they did not report mechanical properties or fracture patterns (Amuda & Mridha, 2009).

On the other hand, the microstructure of the weld metal showed columnar grains but did not show needle of martensite or Laves phases. These results agreed with those reported in the literature (Amuda & Mridha, 2009; Anttila *et al*., 2013; Lakshminarayanan & Balasubramanian, 2012; Ramkumar *et al*., 2015).

The results of this work indicated that sample 3 has the best combination of mechanical properties and elongation. Besides, dimples on the fracture surface of that sample are evidence of a ductile behavior of the weld joint (Wright, 1971). Then, these results indicate that heat input influences the mechanical properties of the welded joints; in this case, the greater the heat input, the coarser the grain size in the HAZ. Moreover, the lowest the heat inputs applied in the welded joint are, the more possibilities are there to find lack of fusion in the weld.

Conclusions

The previously discussed results of this work led to conclude that microstructures in the HAZ of AISI 439 stainless steel showed grain coarsening; a heat input of 172.20 J/mm generated no joint and heat inputs around 295 J/mm generates welds with mechanical properties similar to the properties of the FSS AISI 439, although they even induce grain coarsening in the HAZ. Besides the fracture pattern of the base material consisted of dimples as well as sample 3, which indicated ductility and Quasi-cleavage was found on the fracture surface of the samples, which are located on the filler metals of the specimens, which indicated a brittleness.

Acknowledgements

The authors would like to thank l*aboratorio de metalografía y análisis de falla* of *Centro de Ingeniería y Desarrollo Industrial* for the support during this research.

References

American Society of Testing Materials. (2011). *ASTM-E03-11: Standard Guide for Preparation of Metallographic Specimens.*

American Society of Testing Materials. (2016). *ASTM-E8/E8M–16a: Standard Test Methods for Tension Testing of Metallic Materials.*

American Society of Testing Materials. (2013) *ASTM designation: E112 – 13, Standard Test Methods for Determining Average Grain Size.*

Amuda, M. O. H., Akinlabi, E. T., & Mridha, S. (2017) Influences of Energy Input and Metal Powder Addition on Carbide Precipitation in AISI 430 Ferritic Stainless Steel Welds. Materials Today: *Proceedings, 4*(2), 234-243. doi: https://doi.org/10.1016/j.matpr.2017.01.017

Amuda, M. O. H., & Mridha, S. (2009) Microstructural features of AISI 430 ferritic stainless steel (FSS) weld produced under varying process parameters. *International Journal of Mechanical and Materials Engineering, 4*(2), 160-166.

Amuda, M. O. H., & Mridha, S. (2010) Grain refinement in ferritic stainless steel welds: the journey so far. *Advanced Materials Research, 83*, 1165-1172. doi: https://doi.org/10.4028/www.scientific.net/AMR.83-86.1165

Anttila, S., Karjalainen, P., & Lantto, S. (2013). Mechanical properties of ferritic stainless steel welds in using type 409 and 430 filler metals. *Welding in the World, 57*(3), 335-347. doi: https://doi.org/10.1007/s40194-013-0033-7

Anttila, S., & Porter, D. A. (2014). Influence of shielding gases on grain refinement in welds of stabilized 21% Cr ferritic stainless steel. *Welding in the World, 58*(6), 805-817. doi: http://dx.doi.org/10.1007/s40194-014-0160-9

Chandrakanth, B., Abinesh Kumar, S. V., Ashwin Kumar, S., & Sathish, R. (2014). Optimization and non-destructive test analysis of SS316 weldments using GTAW. *Materials Research, 17*(1), 190-195. doi: http://dx.doi.org/10.1590/S1516-14392013005000188.

Khattak, M. A., Zaman, S., Tamin, M. N., Badshah, S., Mushtaq, S., & Omran, A. A. B. (2017). Effect of Welding Phenomenon on the Microstructure and Mechanical Properties of Ferritic Stainless Steel–A Review. *Journal of Advanced Research in Materials Science, 32*(1), 13-31.

Lakshminarayanan, A. K., & Balasubramanian, V. (2012). Evaluation of microstructure and mechanical properties of laser beam welded AISI 409M grade ferritic stainless steel. *Journal of Iron and Steel Research International, 19*(1), 72-78. doi: https://doi.org/10.1016/S1006-706X(12)60050-8

Lakshminarayanan, A. K., Shanmugam, K., & Balasubramanian, V. (2009). Effect of autogenous arc welding processes on tensile and impact properties of ferritic stainless steel joints. *Journal of Iron and Steel Research International, 16*(1), 62-68. doi: https://doi.org/10.1016/S1006-706X(09)60012-1

Mohandas, T., Reddy, G. M., Naveed, M. (1999). A comparative evaluation of gas tungsten and shielded metal arc welds of a ferritic stainless steel. *Journal of Materials Processing Technology, 94*(2), 133-140. doi: https://doi.org/10.1016/S0924-0136(99)00092-8

Ramkumar, K. D., Chandrasekhar, A., Singh, A. K., Ahuja, S., Agarwal, A., Arivazhagan, N., & Rabel, A. M. (2015). Comparative studies on the weldability, microstructure and tensile properties of autogeneous TIG welded AISI 430 ferritic stainless steel with and without flux. *Journal of Manufacturing Processes, 20*(Part 1), 54-69. doi: https://doi.org/10.1016/j.jmapro.2015.09.008.

Sathish, R., Naveen, B., Nijanthan, P., Geethan, K. A. V., & Rao, V. S. (2012). Weldability and process parameter optimization of dissimilar pipe joints using GTAW. *International Journal of Engineering Research and Applications, 2*(3), 2525-2530.

Silva, L. A., Lima, L. I. L., & Campos, W. R. C. (2007). Microstructural characterization of the HAZ of the AISI 439 with different heat input. *2007 International Nuclear Atlantic Conference INAC 2007*. Santos SP, Brazil.

Teker, T. (2013). Effect of synergic controlled pulsed and manual gas metal ARC welding processes on mechanical and metallurgical properties of AISI 430 ferritic stainless steel. *Archives of Metallurgy and Materials, 58*(4), 1029-1035. doi: https://doi.org/10.2478/amm-2013-0122

Villafuerte, J. C., Kerr, H. W., & David, S. A. (1995). Mechanisms of equiaxed grain formation in ferritic stainless steel gas tungsten arc welds. *Materials Science and Engineering: A, 194*(2), 187-191. doi: https://doi.org/10.1016/0921-5093(94)09656-2

Wright, R. N. (1971). Mechanical behavior and weldability of a high chromium ferritic stainless steel as a function of purity. *Welding Journal, 50*(10), 434-440.

Zaman, S., Khattak, M. A., & Tamin, M. N. (2018), Effects of Welding on the Microstructural Properties of AISI 430 Ferritic Stainless Steel. *Journal of Advanced Research in Materials Science, 44*(1), 25-32.

Zhang, Z., Wang, Z., Wang, W., Yan, Z., Dong, P., Du, H., & Ding, M. (2015). Microstructure evolution in heat affected zone of T4003 ferritic stainless steel. *Materials & Design, 68*, 114-120. doi: https://doi.org/10.1016/j.matdes.2014.12.018